

# Parameter-free Simulation of Photon-detection Probability in CMOS Single-photon Avalanche Diodes

Chin-An Hsieh\* and Sheng-Di Lin.

Institute of Electronics, National Chiao Tung University, 1001 University Road, Hsinchu 300, Taiwan

\*Corresponding Author: [eric50224@gmail.com](mailto:eric50224@gmail.com), telephone: +886-3-5712121#54240

We develop a parameter-free simulation method for predicting photon-detection probability (PDP) of CMOS single-photon avalanche diodes. The method combines TCAD and trigger probability calculation to simulate PDP spectra at all excess voltages so is useful for device design and optimization. Consistent results between our theory and experiment are presented.

## I. Introduction

Due to their single-photon sensitivity, excellent timing resolution and readiness for on-chip integration with CMOS circuits, weak-light detection using single-photon avalanche diodes (SPADs) have been used in areas such as fluorescence lifetime imaging microscopy [1] [2], light detection and ranging (LiDAR) [3], and time-gated Raman spectroscopy [4]. In particular, the strong demand for ranging in advanced driver assistance systems and autonomous driving requires high-resolution images and precise distance measurements with low laser power for eyes safety consideration. Therefore, the improvement of the SPAD's photon detection probability (PDP) becomes an important issue. However, quantitative prediction of PDP has been a difficult task due to its complicated factors, including detailed doping distribution, carrier transport above breakdown voltage, non-uniform electric field and impact ionization distribution, and spatially-dependent breakdown triggering probability. Recently, Pancheri *et al.* compared two breakdown models to simulate PDP spectra and their dependence on the excess bias voltage of SPADs [5]. However, they used a few parameters in their fitting, which would make a correct quantitative prediction not possible in device design and optimization. In this report, we propose and develop a parameter-free simulation method to predict PDP of CMOS SPADs based on fabrication processing parameters. By combining TCAD with position-dependent breakdown-triggering probability calculation, the voltage-dependent PDP spectra have been simulated. Comparison between theory and experiment is presented.

## II. Device Design and Measurement

We fabricate, characterize, and simulate SPAD in Episcil 0.8- $\mu\text{m}$  standard CMOS technology. Figure 1 illustrates the device structure. The P-N junction is formed by PPLUS and NWELL layers with PWELL layer as a guard ring. With all the detailed process parameters from Episcil, we start with process simulation using SPROCESS module in Synopsys Sentaurus

TCAD to obtain 2-D doping profiles, as shown in Fig. 2. Figure 3 shows the schematic on-chip circuit. An NMOS serves as a passive quenching circuit, and the anode is connected to an inverter and a buffer for signal output. The measured breakdown voltage is about 28.0 V Up to 40 V, the dark count rate is a few hundred Hz as shown in Fig. 4.

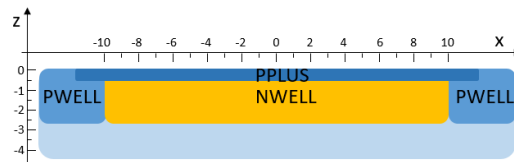


Fig. 1 Schematic SPAD device structure

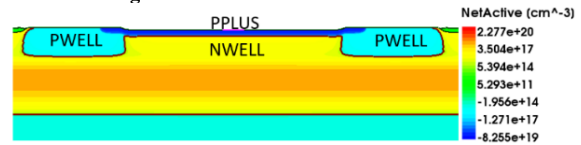


Fig. 2 Simulated 2-D doping distribution

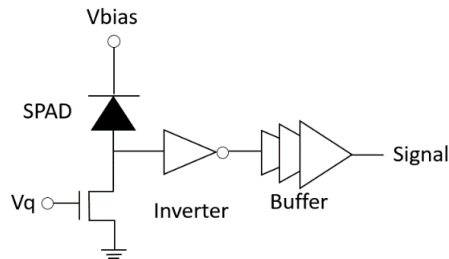


Fig. 3 Schematic SPAD circuit

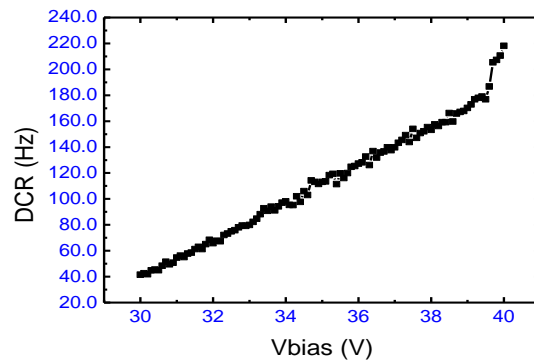


Fig. 4 Dark count rate

To characterize the PDP of SPADs in a dark box, photons from a halogen light source (ORIEL-66188) were first dispersed by a monochromator (HR-550) and then coupled into an integrating sphere via a large-core fiber. The SPADs and the calibrated photodiode (Thorlabs FDS100-CAL) were illuminated at the same time through the two holes on the integrating sphere. The incident photon flux is real-time monitored by the photodiode to calculate the incident photon number per unit area on SPADs. A shutter in front of monochromator was switched on and off in turns so the light and dark counts can be measured under the same condition.

### III. Device Design and Measurement

We develop a simulation procedure combining TCAD with triggering probability calculation to predict PDP. Considering a PPLUS/NWELL SPAD, the PDP spectra can be calculated by,

$$\text{PDP}(\lambda) = (1 - R(\lambda)) \int_{z_p}^{z_n} \alpha_s \exp(-\alpha_s z) P_{total}(z) dz, + I_{ph}^e P_e(z_p) + I_{ph}^h P_h(z_n) \quad (1)$$

where  $R(\lambda)$  is the surface reflectivity.  $\alpha_s(\lambda)$  is the absorption coefficient of silicon at wavelength of  $\lambda$ .  $z_n$  and  $z_p$  are the respective depletion edge on the n- and p-side.  $P_{total}(z)$  is the breakdown probability triggered by electrons or holes photo-generated at  $z$  position [1].  $P_e(z_p)$  ( $P_h(z_n)$ ) is breakdown probability triggered by

electrons (holes) at p-side (n-side) depletion edge.  $I_{ph}^e$  ( $I_{ph}^h$ ) is the single-photon generated electron (hole) first term in equation (1) means the part of PDP contributed from the electron-hole pairs which generated in the depletion region, the second and third term are contributed from the electrons (holes) generated in PPLUS (NWELL) neutral region and diffusing to depletion region.

We use the van Overstraeten-de Man model for impact ionization coefficient [6] Local-field model is applied to calculating the self-consistent trigger breakdown probability of electrons ( $P_e(z)$ ) and holes ( $P_h(z)$ ) in the depletion region by solving the following equation [7],

$$\frac{dP_e}{dx} = -(1 - P_e)\alpha_e[P_e + P_h - P_e P_h] \quad (2a)$$

$$\frac{dP_h}{dx} = (1 - P_h)\alpha_h[P_e + P_h - P_e P_h] \quad (2b)$$

so  $P_{total} = P_e + P_h - P_e P_h$  can be obtained.

We use SDEVICE module in Synopsys Sentaurus TCAD for electric field simulation at all voltages, including that above breakdown voltage shown in Fig. 5 by turning off the impact ionization. Figure 6 shows the vertical E-field distribution at edge ( $x = 8 \mu\text{m}$ ) is wider and the maximum is much lower than those at center ( $x = 0 \mu\text{m}$ ). The horizontal E-field distribution at various position in Fig. 7 confirms this observation, which will be taken into account for PDP calculation later in this report.

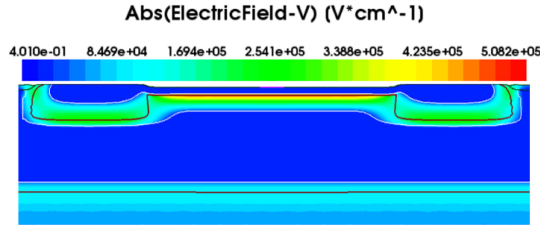


Fig. 5 Simulated 2-D electric field distribution at  $V = 30 \text{ V}$ .

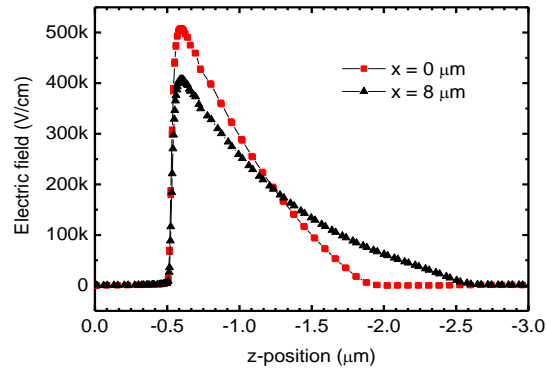


Fig. 6 Vertical E-field distributions at two positions.

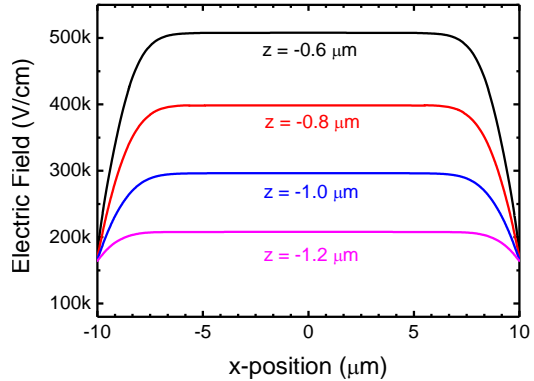


Fig. 7 Horizontal E-field distributions at various depths.

With E-field at various voltages, the 1-D trigger probability is solved accordingly at various x-positions. Figures 8 and 9 respectively exhibit those at  $x = 0 \mu\text{m}$  and  $x = 8 \mu\text{m}$  at  $30 \text{ V}$ , showing a much higher triggering probability at the centered region. The non-uniform E-field distribution causes the dramatic decrease of PDP at the device edge.

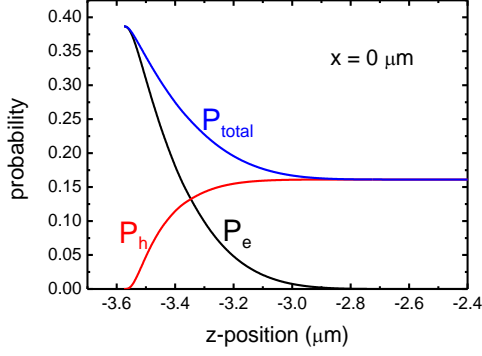


Fig. 8 Simulated trigger probability at center

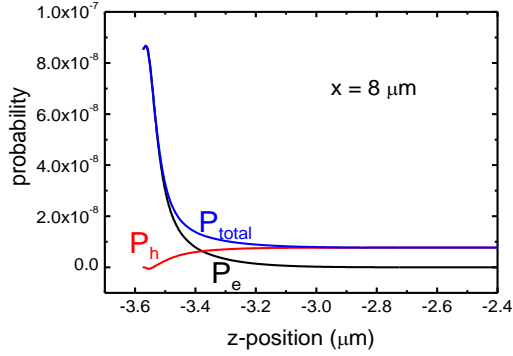


Fig. 9 Simulated trigger probability at edge

Our simulation continues with the optical simulation in TCAD to obtain the optical generated electron and hole currents, to extract  $I_{ph}^e$  and  $I_{ph}^h$  in equation (1), as the device is illuminated by photons at a fixed wavelength. Figures 10 and 11 respectively illustrate the optical generation obtained by SDEVICE in which the device is illuminated by 500-nm and 900-nm photon flux of  $0.05 \text{ W/cm}^2$ . As expected, the distribution of photon generation rate decays fast in Fig. 10 due to the large absorption coefficient of silicon at 500 nm,  $\sim 1.11 \times 10^4 \text{ cm}^{-1}$ . In contrast, at 900 nm, the distribution is much more uniform in depth. By simulation of optical generation at all wavelengths, finally, the PDP spectra at a fixed voltage are obtained with equation (1) if surface reflection is known. To calculate bias-dependent PDP, we simply used the same optical generation distribution and repeated the calculation.

#### IV. Results and Discussions

Figure 12 shows the simulated and measured bias-dependent PDP at the wavelengths of 500, 700 and 900 nm. Highly consistent results have been obtained between theoretical calculation and experimental data. Note that the theoretical bias-dependent PDPs were normalized to the measured ones at the highest voltage because the reflectivity spectra is not available in these devices. Figure 13 shows the simulated PDP at 500 nm

as a function of  $x$ . We can see that the PDP for  $x$  less than  $6 \mu\text{m}$  is quite uniform but drops very fast to nearly zero at  $x = 8 \mu\text{m}$  due to the vanishing trigger probability at device edge (Fig. 9). Experimental and theoretical PDP spectra considering this PDP non-uniformity are plotted in Fig. 14. In this simulation, the reflectivity only arises from silicon-air interface so there is no oscillation in the simulated PDP spectra and a slight difference between experiment and simulation do exist.

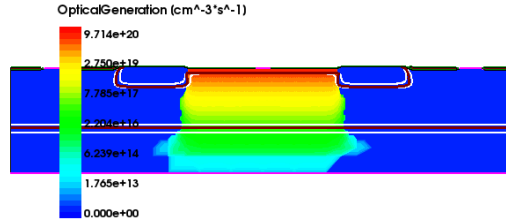


Fig. 10 Simulated optical generation when illuminated 500-nm photons

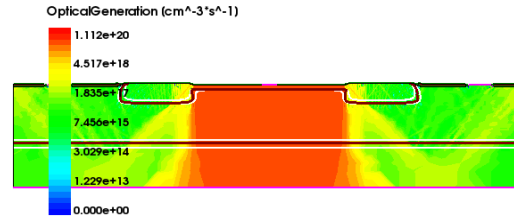


Fig. 11 Simulated optical generation when illuminated 900nm photons

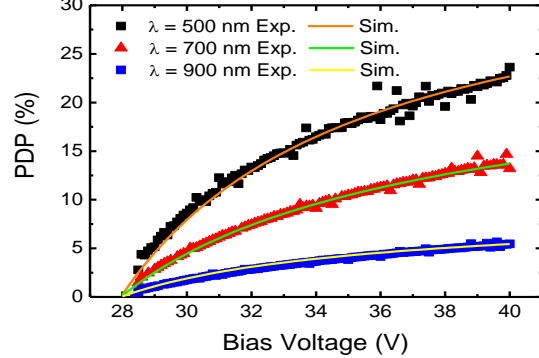


Fig. 12 Simulated and measured bias-dependent PDP at various wavelength

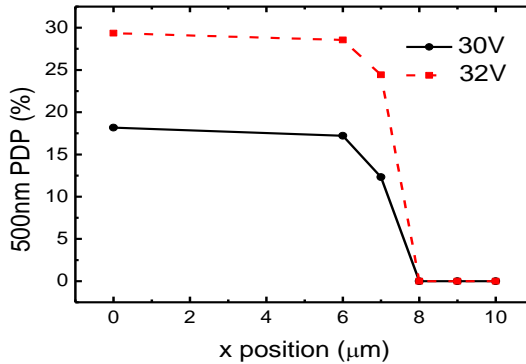


Fig. 13 Simulated 500nm PDP at various position

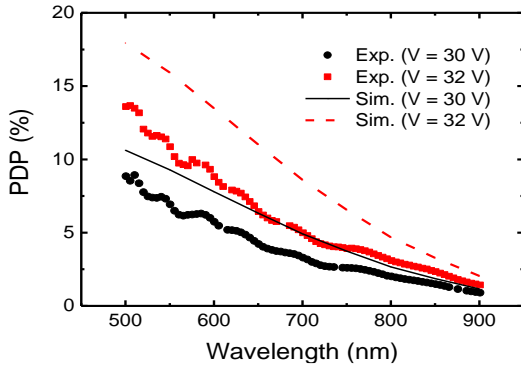


Fig. 14 Simulated and measured PDP spectra at two bias voltages

## V. Conclusion

A parameter-free simulation scheme to calculate PDP of CMOS SPAD is presented. Combining processing, electrical, optical simulation modules in TCAD and the self-consistent solution of triggering probability distribution of avalanche breakdown, we can not only simulate bias-dependent PDP spectra but also take the E-field non-uniformity into account. Our results show an excellent consistence between simulation and experiment. It is also revealed that the uniformity problem seriously lowers the PDP of SPADs, and it would become a key issue in device scaling down in the future.

**Acknowledgement:** We thank the financial support from MOST in Taiwan. We are grateful to the National Center for High-performance Computing for computer time and facilities and Episil Corp. Ltd. for their help on chip fabrication.

## References

- [1] D. E. Schwartz, E. Charbon, and K. L. Shepard, "A single-photon avalanche diode array for fluorescence lifetime imaging microscopy," *IEEE J. Solid-State Circuits*, vol. 43, no. 11, pp. 2546–2557, Nov. 2008.
- [2] D. U. Li, J. Arlt, J. Richardson, R. Walker, A. Buts, D. Stoppa, E. Charbon, and R. Henderson, "Real-time fluorescence lifetime imaging system with a 32 x 32 0.13 $\mu$ m CMOS low dark-count single-photon avalanche diode array," *Opt. Express*, vol. 18, no. 10, pp. 10257–10269, 2010.
- [3] C. Niclass, M. Soga, H. Matsubara, M. Ogawa, and M. Kagami, "A 0.18- $\mu$ m CMOS SoC for a 100-m-range 10-frame/s 200x96-pixel time-of-flight depth sensor," *IEEE J. Solid-State Circuits*, vol. 49, no. 1, pp. 315–330, Jan, 2014.
- [4] J. Blacksberg, Y. Maruyama, E. Charbon, and G. R. Rossman, "Fast single-photon avalanche diode arrays for laser Raman spectroscopy," *Opt. Lett.* vol. 36, no. 18, pp. 3672–3674, Sep. 2011.
- [5] L. Pancheri, D. Stoppa, and G-F Dalla Betta, "Characterization and Modeling of Breakdown Probability in Sub-Micrometer CMOS SPADs.," *IEEE Journal of Selected Topics in Quantum Electronics*, vol. 20, no. 6, pp.328-335, Nov. 2014.
- [6] R. Van Overstraeten and H. De Man, "Measurement of the ionization rates in diffused silicon p–n junctions," *Solid-State Electron.*, vol. 13, pp. 583–608, 1970.
- [7] W. G. Oldham, R. R. Samuelson, and P. Antognetti, "Triggering phenomena in avalanche photodiodes," *IEEE Trans. Electron. Devices*, vol. ED-19, no. 9, pp. 1056–1060, Sep. 1972.